IJNAOE
©SNAK, 2015

Int. J. Nav. Archit. Ocean Eng. (2015) 7:399~408
http://dx.doi.org/10.1515/ijnaoe-2015-0028
pISSN: 2092-6782, eISSN: 2092-6790

Ultimate uniaxial compressive strength of stiffened panel with opening under lateral pressure

Chang-Li Yu[1,2], Ji-Cai Feng[2] and Ke Chen[3]

[1]*School of Naval Architecture, Harbin Institute of Technology, Weihai, China*
[2]*Post-Doctoral Station of Materials Science and Engineering, Harbin Institute of Technology, Harbin, China*
[3]*China Shipping Container Lines Co., Ltd., Shanghai, China*

ABSTRACT: *This paper concentrated on the ultimate uniaxial compressive strength of stiffened panel with opening under lateral load and also studied the design-oriented formulae. For this purpose, three series of well executed experiments on longitudinal stiffened panel with rectangular opening subjected to the combined load have been selected as test models. The finite element analysis package, ABAQUS, is used for simulation with considering the large elasticplastic deflection behavior of stiffened panels. The feasibility of the numerical procedure is verified by a good agreement of experimental results and numerical results. More cases studies are executed employing nonlinear finite element method to analyze the influence of design variables on the ultimate strength of stiffened panel with opening under combined pressure. Based on data, two design formulae corresponding to different opening types are fitted, and accuracy of them is illustrated to demonstrate that they could be applied to basic design of practical engineering structure.*

KEY WORDS: Ultimate strength; Stiffened panel; Rectangular opening; Combined load; Design formulae fitting.

INTRODUCTION

Due to simplicity in their fabrication and excellent strength-to-weight ratio, stiffened panel is used extensively for naval architecture and ocean engineering. Opening is necessitated by piping, ducts and other accessories for maintenance purposes. A ship deck composed by stiffened panel with a square opening under typical loads is shown in Fig. 1. The deck stiffened panel is subjected a constant lateral load due to the cargo while the bottom shell is under buoyant force. The deck and bottom shell of a ship's hull are also subjected to compressive stress due to sagging or hogging bending moments. Ultimate limit state, fatigue limit state, accidental limit state and serviceability limit state are four types of limit states which are usually taken into account during structure design. Among them, design based on ultimate strength has been considered as an important basis of rational design by International Association of Classification Societies (IACS) (2008). Therefore, this paper is concerned with ultimate strength of stiffened panel with opening under combined load of uniaxial compression and lateral pressure.

It is evident that opening reduces the ultimate strength of stiffened panel, and a lot of literatures on the ultimate strength of plate with different types of openings subjected to various load are described. Roberts and Azizian (1984) generated interaction curves for ultimate strength of square plates with central square and circular holes subjected to uniaxial compression,

Corresponding author: *Chang-Li Yu*, e-mail: *yuchangli@hitwh.edu.cn*

biaxial compression and pure shear. Narayanan and Chan (1985) presented design charts based on ultimate strength of plate containing circular holes under linearly varying edge displacements. Jwalamalini et al. (1992) developed the design charts for the stability of simply supported square plate with opening under in-plane loading as uniform compression and trapezoidal loads. Madasamy and Kalyanaraman (1994) presented the analysis of plated structures with rectangular cutouts and internal supports using the spline finite strip method. Paik et al. (2001) presented ultimate strength formulations for ship plating under combined biaxial compressions/tension, edge shear, and lateral pressure loads. Bambach and Rasmussen (2002) carried out the test of unstiffened elements under different combined compression and bending cases. Khaled et al. (2004) employed finite element method to determine the elasto-plastic buckling stress of uniaxial loaded simply supported square and rectangular plates with circular openings. Suneel Kumar et at. (2009) determined the ultimate strength of ship deck plating with a circular opening extended to full width between stiffeners subjected to axial and lateral loads. Mohtaram et al. (2011) carried out the experimental and numerical investigation of buckling in rectangular steel plates with groove-shape cut out and clamped supported at upper and lower ends and free supported in the other ends. Yu and Lee (2012) determined the design formula for ultimate compressive strength of simply supported unstiffened plate with opening. A critical review of literature indicated that there is no design reference reported on the ultimate strength of stiffened panel with rectangular opening under combined load of compression and lateral pressure.

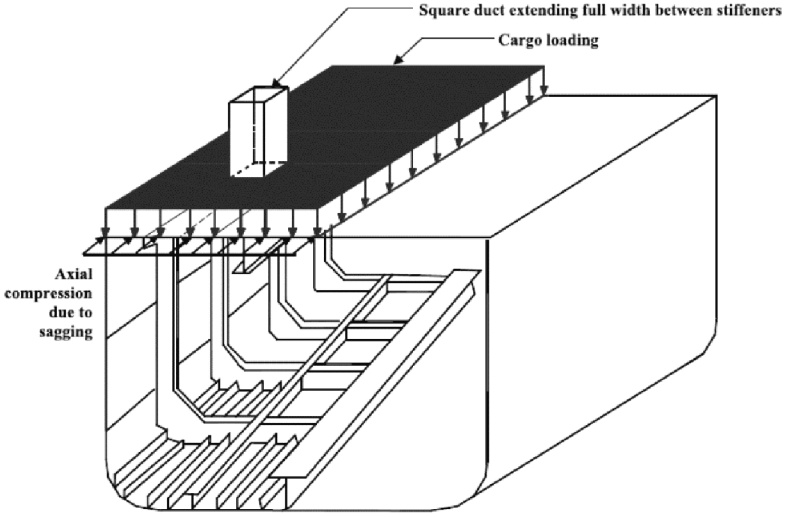

Fig. 1 A typical stiffened panel with rectangular opening.

VERIFICATION MODEL

Suneel et al. (2009) carried out an experiment to test the behaviors of stiffened panel with opening under both axial and lateral loads. Three stiffened plate specimens with a square opening at the center of each specimen in between the stiffeners were fabricated. Four longitudinal angle stiffeners were connected to the flange plate of each specimen through continuous welding. The dimensions of all parts are shown in Fig. 2. A square opening was made at the center of the stiffened plate by drilling, gas cutting and filing. The modulus of elasticity (E) and yield stress (σ_y) of the material were 1.98×10^5 *MPa* and 331 *MPa*, respectively. The yield strain and Poisson's ratio were found to be 3700 microns and 0.3, respectively. There were three specimens with same measure and material, but they were subjected to different load cases and denoted in Table 1.

The plating in ships is usually continuously welded along the plate-stiffener intersection and it is well established that the welding process introduces a residual stress field and an associated initial distortion in the plate and stiffener. The initial geometrical imperfections and residual stresses influence significantly the ultimate strength of stiffened panels. The initial imperfections in the stiffened panel, classified as (1) imperfection in the plate (Δ_x), (2) overall imperfection of the whole panel (Δ_{sx}) and (3) torsional imperfection in stiffeners (Δ_{sy}), which are shown in Fig. 3, were measured in all fabricated test panels and summarized in Table 1. The residual stresses developed due to continuous welding of stiffeners to the flange plate and due to gas cutting for opening are not in the scope of the present study and hence were not considered in the numerical analysis.

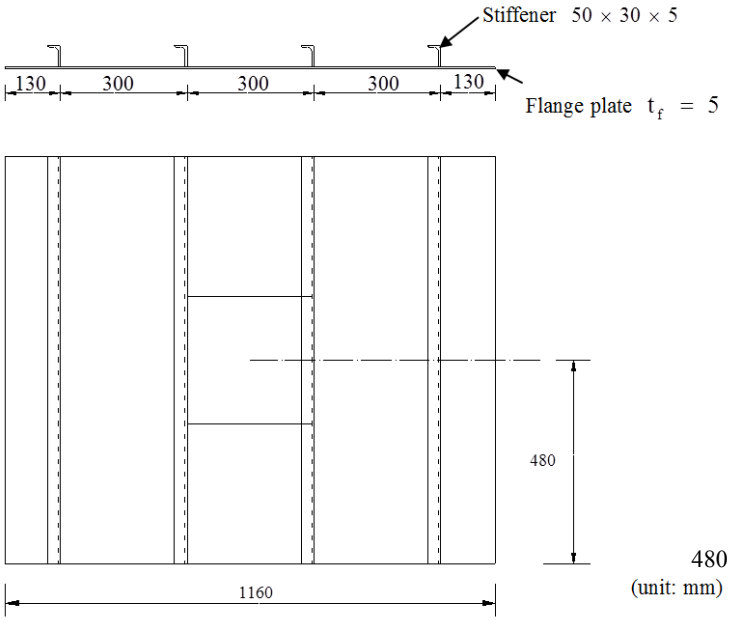

Fig. 2 Stiffened panel with opening.

Table 1 Specimens and their initial imperfection.

Serial no.	Specimen	Constant lateral load (q) kN/m^2	Measured imperfections (mm)		
			Δ_x	Δ_{sx}	Δ_{sy}
1	STPO1	0	+0.219	+0.554	-0.800
2	STPO2	90	+0.251	+0.815	+0.735
3	STPO3	180	+0.333	+0.145	+0.735

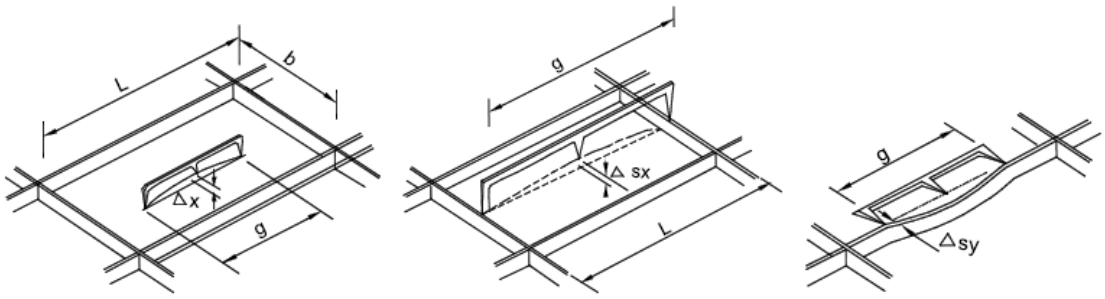

(a) Plate imperfection. (b) Overall imperfection. (c) Stiffener imperfection.

Fig. 3 Initial imperfections.

The finite element analysis package, ABAQUS, was used for modeling, analysis and post processing of stiffened panel with rectangular opening. "Buckle" step was completed to simulate the initial imperfection, and "Static, General" was executed simultaneously if there was lateral load. The displacement results in above two steps were read and loaded during nonlinear calculation step "Static, Riks" (Arc Length Method) by editing keywords of command stream. Both geometric and material nonlinearities were considered in the analysis. Large displacement option was activated in geometric nonlinear analysis. Material nonlinearity was modeled using an incremental plasticity theory assuming the material to be ideal elastic-plastic. Maximum number of increments was 100, initial and minimum values of "Arc length increment" were 0.1 and 1e-12 respectively. The mesh size was selected as 25 *mm* × 25 *mm* considering the calculation convergence and consuming time, more details can be found in reference (Suneel et al., 2007). A typical finite element mesh used in the present analysis is shown in Fig. 4, the

stiffened panel were discretized into 8 node quadrilateral elements. The element has six degrees of freedom at each node: three translations (u_x, u_y and u_z) and three rotations (UR_x, UR_y and UR_z). Boundary condition is shown in Fig. 5. One hand, all the nodes in edges parallel to stiffener were restrained for deflection in all direction except Y direction and rotation in all direction. On the other hand, all the nodes in edges perpendicular to stiffeners were beam type MPC constrained in one reference point, in which the displacement loading is applied. Deflections in X and Z directions were restrained and rotation around Y and Z axis were fixed to zero. Out-of-plane uniform pressure was applied on the structure.

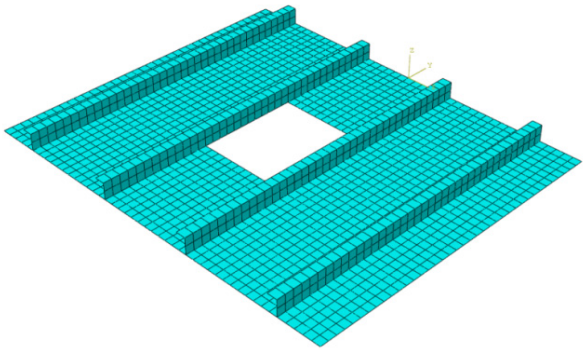

Fig. 4 Typical finite element mesh.

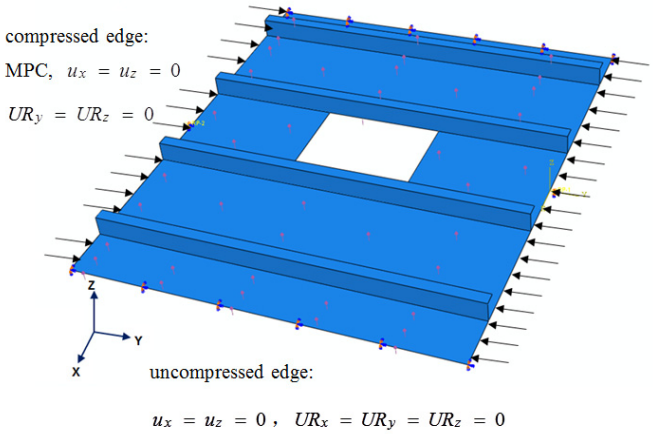

Fig. 5 Boundary conditions.

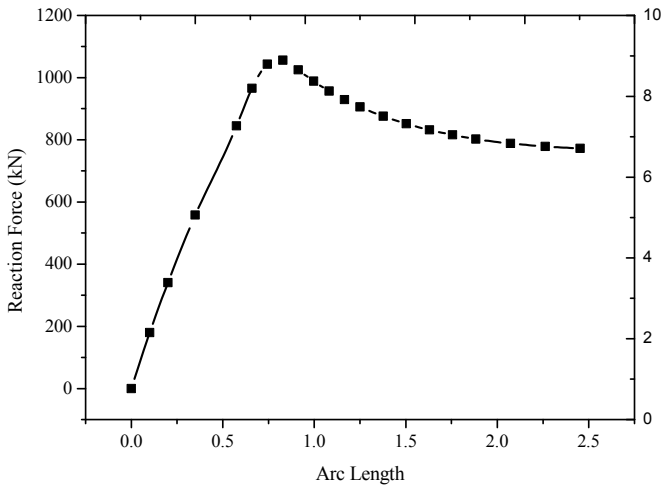

Fig. 6 Typical plot of axial reaction force/arc length for STPO2.

A typical plot of axial reaction force/arc length for specimen STPO2 is shown in Fig. 6, and ultimate load-carrying capacity is defined as the peak point. The comparison of ultimate uniaxial compression-carrying capacity between experimental results and FEM results is shown in Table 2. The differences of numerical results and experimental results are below 1.5% that verifies numerical analysis procedure.

Table 2 Comparison FEM results with experimental results

Specimen	Experimental results U_{ex} (*kN*)	FEM results U_{fe} (*kN*)	Difference
STPO1	1248.32	1251.34	0.2%
STPO2	1049.77	1038.82	1.04%
STPO3	828.31	839.71	1.38%

CASES STUDY

The unit panel consisting of a flange plate equal to the width of the plate between the stiffeners and a stiffener attached to it considered for the parametric study. The plating thicknesses of models were selected as 5 *mm*, 8 *mm*, 10 *mm*, 12 *mm*, 15 *mm* and plate slenderness ratio ($\beta = s/t_f \sqrt{\sigma_y/E}$) was 2.45, 1.53, 1.23, 1.02 and 0.8, respectively. The ultimate strength of structure (σ_u), which was subjected to combined loads of axial compression and constant lateral loads, was defined as the ratio of ultimate compression-carrying capacity of structure and cross-sectional area of stiffened panel. The normalized ultimate strength parameter is defined as $\sigma_n = \sigma_u/\sigma_y$. The lateral loads of $Q = q_u/6, q_u/3, q_u/2, 2q_u/3, 5q_u/6$ were considered in this study. q_u is the ultimate lateral load-carrying of specimen, which is 341.3 kN/m^2 obtained by experiment (Suneel et al., 2009). The normalized lateral load Q_n is calculated as $Q_n = QE/(\sigma_y)^2$ Guedes Soares and Gordo, 1996, which was 0.103, 0.206, 0.308, 0.411 and 0.514 respectively. Two types opening cases, as shown in Fig. 7, were considered to study the influence of opening area on the structural ultimate strength: one type is opening width is fixed as 300 *mm* and opening depth is changed as 150 *mm*, 300 *mm*, 450 *mm* and 600 *mm*; another type is opening depth is constant of 300 *mm* and opening width is 100 *mm*, 200 *mm* and 300 *mm*, respectively. The normalized opening area parameter α is defined as the area ratio of opening and plate between stiffeners, so α is 0.156, 0.313, 0.469 and 0.625 for type 1 opening, 0.104, 0.208 and 0.313 for type 2 opening in present study.

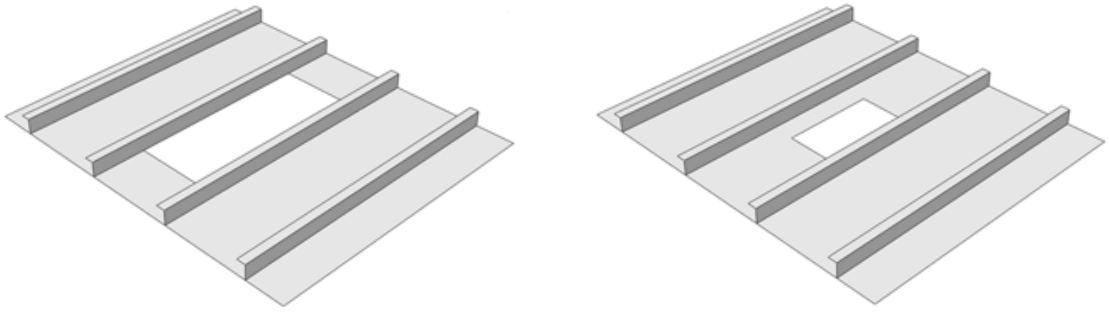

(a) Type 1 opening. (b) Type 2 opening.

Fig. 7 Opening cases.

Regarding models with type 1 opening, a typical plot of normalized ultimate strength parameter σ_n with opening area parameter α and normalized lateral load Q_n in the case of model plate slenderness ratio $\beta = 2.45$ is shown in Fig. 8. The variation of σ_n with α in Fig. 8 (a) is almost flat and the maximum difference of σ_n between different α is around 9%, which indicates that there is a little influence of opening area to the ultimate strength of models with type 1 opening. That may because the plating, where opening locates on, offers a little contribution to ultimate axial compression-carrying capacity when the opening area exceeds a certain level. Therefore, for a fix Q_n, the average of σ_n corresponding to different α is selected as

representative normalized ultimate strength. In contrast, Fig. 8 (b) shows that the change of σ_n with Q_n is almost linear. In other words, lateral load linearly decreases the ultimate strength of models with type 1 opening. The relation of average σ_n and β for different Q_n is drawn in Fig. 9. The average normalized ultimate strength σ_n changes with β in an exponential trend. All the data for other thickness models show similar trends and the results are summarized in Table 3.

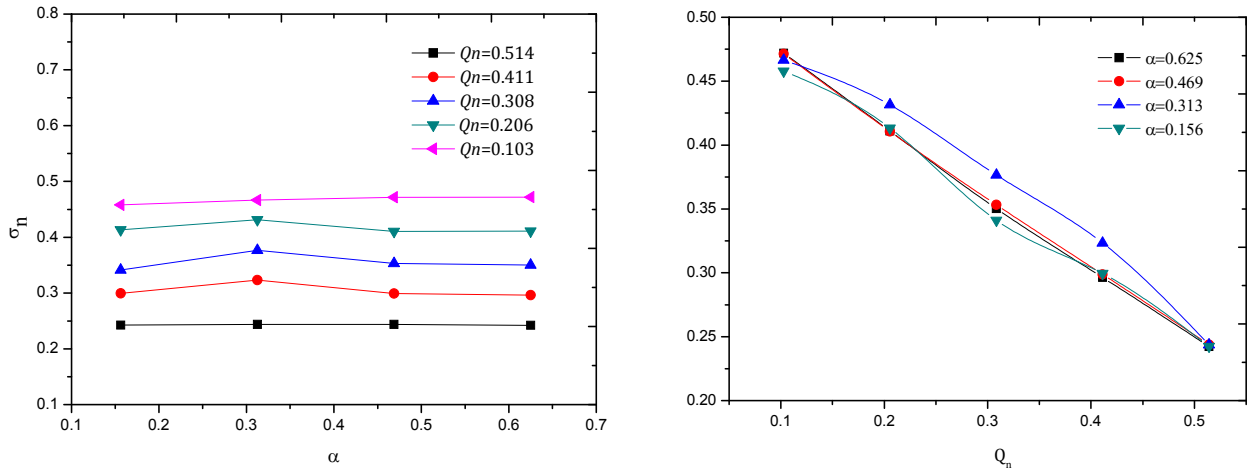

(a) σ_n versus α. (b) σ_n versus Q_n.

Fig. 8 Relation of σ_n with α and Q_n in the case of $\beta = 2.45$ for models with type 1 opening.

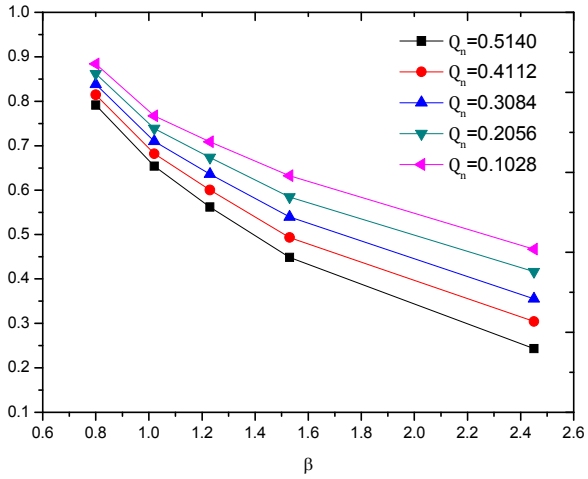

Fig. 9 Relation of average σ_n and β for models with type 1 opening.

Table 3 Numerical results of models with type 1 opening.

β	σ_n				
	$Q_n = 0.103$	$Q_n = 0.206$	$Q_n = 0.308$	$Q_n = 0.411$	$Q_n = 0.514$
2.45	0.4669	0.4166	0.3553	0.3045	0.2431
1.53	0.6135	0.5730	0.5326	0.4921	0.4516
1.23	0.7067	0.6721	0.6376	0.6030	0.5684
1.02	0.7861	0.7557	0.7253	0.6948	0.6644
0.8	0.8818	0.8557	0.8296	0.8036	0.7775

σ_n/α and σ_n/Q_n curves in the case of $\beta = 2.45$ for the test models with type 2 opening are drawn in Fig. 10. The curve of σ_n/α in Fig. 10 (a) indicates that the opening area significantly affects the ultimate strength of models with type 2 opening as the lateral load is not large, the maximum difference is about 25%. In the low lateral load condition, the relation of ultimate strength and opening area is nonlinear. However, when the lateral load is large enough, the impact of opening area on ultimate strength can be neglected compared to that of lateral load. The relation of ultimate strength and lateral load could be approximately considered as linear from the curve of σ_n/Q_n in Fig. 10 (b). The relation between ultimate strength and plating thickness in the case of opening area parameter $\alpha = 0.104$ for models with type 2 opening, σ_n changes with β in a nonlinear trend is shown in Fig. 11. The trends shown from the data for other models are similar and the results are summarized in Table 4.

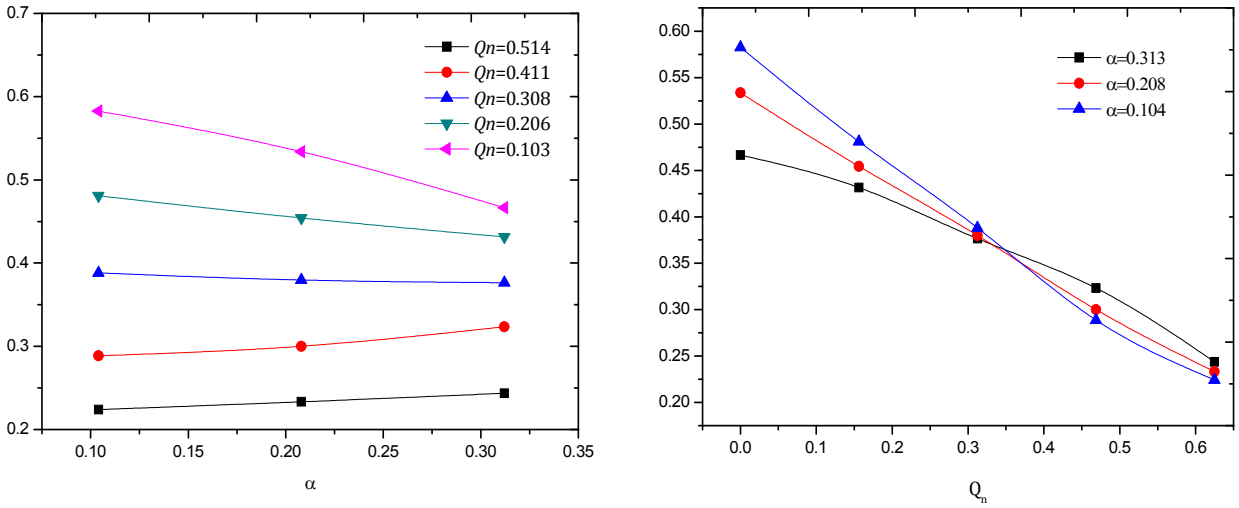

(a) σ_n versus α. (b) σ_n versus Q_n.

Fig. 10 Relation of σ_n with α and Q_n in the case of $\beta = 2.45$ for models with type 2 opening.

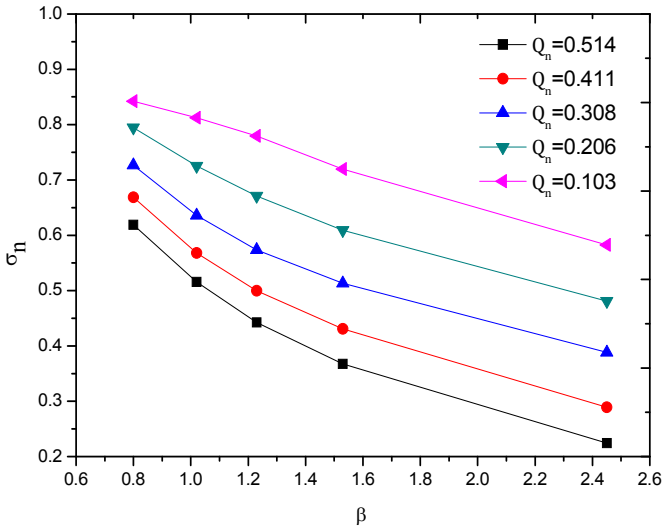

Fig. 11 Relation of σ_n and β in the case of $\alpha = 0.104$ for models with type 2 opening.

Table 4 Numerical results of models with type 2 opening.

β	α	σ_n				
		$Q_n = 0.103$	$Q_n = 0.206$	$Q_n = 0.308$	$Q_n = 0.411$	$Q_n = 0.514$
2.45	0.104	0.5826	0.4810	0.3880	0.2888	0.2241
	0.208	0.5337	0.4543	0.3798	0.3002	0.2333
	0.312	0.4665	0.4315	0.3767	0.3233	0.2437
1.53	0.104	0.7195	0.6093	0.5130	0.4310	0.3678
	0.208	0.6598	0.5843	0.5142	0.4448	0.3810
	0.312	0.5825	0.5280	0.4737	0.4270	0.3797
1.23	0.104	0.7795	0.6711	0.5736	0.4996	0.4424
	0.208	0.7273	0.6624	0.5823	0.5124	0.4529
	0.312	0.6630	0.6056	0.5555	0.5071	0.4611
1.02	0.104	0.8121	0.7252	0.6360	0.5681	0.5155
	0.208	0.7827	0.72252	0.6465	0.5782	0.5235
	0.312	0.7116	0.6753	0.6332	0.5909	0.5460
0.8	0.104	0.8421	0.7945	0.7265	0.6684	0.6191
	0.208	0.8211	0.7831	0.7270	0.6738	0.6244
	0.312	0.7593	0.7364	0.7113	0.6767	0.6391

DESIGN FORMLAE FITTING

Empirical formulae are significant when the basis of theory is still impractical for engineering products design. In this study, the design formulae fitting were carried out following this two aspects:

1) Design formulae have enough accuracy to express the relations between design variables.
2) On the premise of above aspect, expression of design formulae should be as simple as possible in the view of practical engineering application.

Some MATLAB functions were adopted to achieve design formulae fitting. As discussed early, the ultimate strength of models with type 1 opening mainly depends upon lateral load and plating thickness, so "Surface Fitting Tool" command of MATLAB is expedient. The type of fitted equation is polynomial, the highest order of β and Q_n is 2 and 1, respectively. However, the influence of all design variables (plating thickness, lateral load and opening area) on ultimate compression-carrying capacity could not be neglected for models with type 2 opening. Therefore, the command of "Response Surface Tool" in MATLAB is applied and the polynomial type is "Pure Quadatic" to reduce the number of expression. Meanwhile, "Root-Mean-Square Error" (RMSE) is selected to evaluate the effect of fitting function.

The fitted design formula for ultimate strength of structures with type 1 opening under combined load of lateral pressure and uniaxial compression is in Eq. (1). σ_{nn} is denoted as normalized ultimate compressive strength obtained by design formula. RMSE of Eq. (1) is 0.011 that means its accuracy is high enough. In order to illustrate the formula fitting effect more clearly, the comparison between numerical results and design formula is drawn in Figs. 12 and 13. The dots in Fig. 12 are numerical results and the surface is the field covered by Eq. (1) as well. The coordinate points, composed by (σ_n,σ_{nn}) in Fig. 13, are distributed around diagonal line.

$$\sigma_{nn} = 0.132\beta^2 - 0192\beta \bullet Q_n - 0.656\beta - 0.100Q_n + 1.348 \quad (1)$$

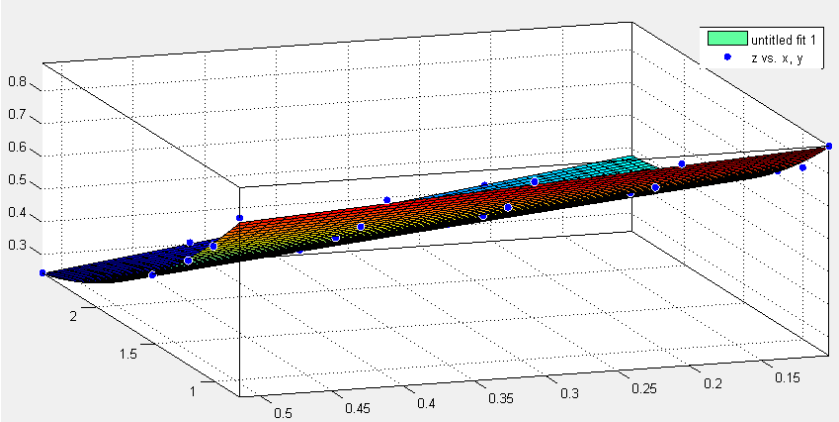

Fig. 12 Comparison of numerical results and Eq. (1).

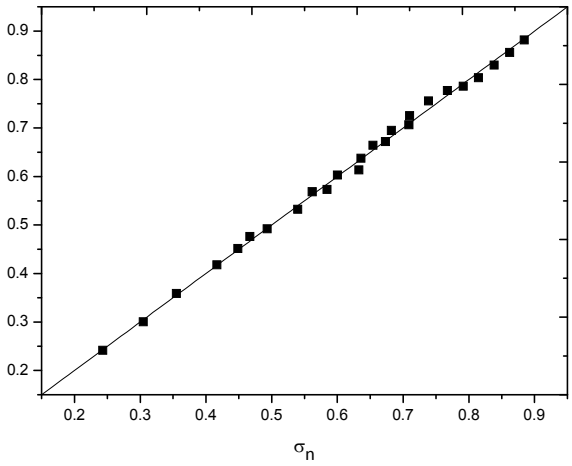

Fig. 13 Distribution of coordinate points (σ_n, σ_{nn}) for models with type 1 opening.

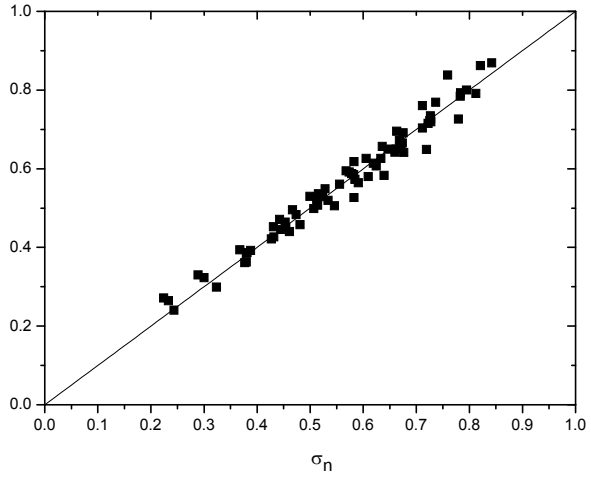

Fig. 14 Distribution of coordinate points (σ_n, σ_{nn}) for models with type 2 opening.

Eq. (2) is the fitted design formula for ultimate strength of structures with type 2 opening under combined load of lateral pressure and uniaxial compression, its RMSE is 0.027. The plot of coordinate points (σ_n, σ_{nn}) is in Fig. 14, all points are also distributed around diagonal line.

$$\sigma_{nn} = 0.102\beta^2 - 0.788\alpha^2 + 0.165Q_n^2 - 0.539\beta + 0.180\alpha - 0.722Q_n + 1.1297 \quad (2)$$

CONCLUSION

This paper is concerned with the ultimate strength of stiffened panel with rectangular opening subjected to combined load of lateral pressure and uniaxial compression. Validity of the present numerical procedure has been verified through comparing the numerical results with well-executed experimental results. And the difference of ultimate compression-carrying capacity is only around 1%. Numerical analysis has been carried out for 100 models with type 1 opening and 75 models with type 2 opening with varying plate thickness, opening area and lateral load. As far as the present numerical analysis, the results are concerned. Regarding different opening area parameter, the error of normalized ultimate strength for the models with type 1 opening is within 9%. As a result, for models with type 1 opening, the influence of opening area on ultimate compressive strength is neglected. In contrast, the effect of opening area on ultimate uniaxial compressive strength is nearly 25%, which means normalized opening area parameter should be considered during design formula fitting of normalized ultimate uniaxial compressive strength. Furthermore, σ_n / Q_n curve is almost linear but σ_n / β curve is nonlinear. Two design formulae expre-

ssing ultimate strength that corresponding to structure with different opening types are fitted by MATLAB function, and RMSE is calculated to evaluate their accuracy. RMSEs of Eqs. (1) and (2) are 0.011 and 0.027 respectively, which demonstrated that the proposed design formulae in this paper could be applied to guide basic design of practical engineering structure.

ACKNOWLEDGEMENTS

This research was supported by HIT Discipline Guide Fund (Project No. : WH20140102).

REFERENCE

Bambach, M.R.BE and Rasmussen, K.J.R.MS., 2002. Tests of unstiffened elements under combined compression and bending. *Research Report No R818 of the University of Sydney*. Sydney: University of Sydney.

Guedes, S.C. and Gordo, J.M. 1996. Collapse strength of rectangular plates under transverse compression. *Journal of constructional steel research*, 36(3), pp.216-234.

IACS, 2008. *Common structure rules for double hull oil tankers,* July. [online] Available at: < http://www.iacs.org.uk/ publications/ CommonRulesDoc.aspx?pageid=4&sectionid=2&linkid=2> [Accessed 30 January 15].

Jwalamalini, R., Sundaravadivelu, R., Vendhan, C.P. and Ganapathy, C., 1992. Stability of initially stressed square plates with square openings. *Marine Structures*, 5(1), pp.71-84.

Khaled, M.El.S., Aly, S.N. and Mohammad, I., 2004. Elasto-plastic buckling of perforated plates under uniaxial compression. *Thin-Walled Structures*, 42(8), pp.1083-1101.

Madasamy, C.M. and Kalyanaraman, V., 1994. Analysis of plated structures with rectangular cutouts and internal supports using the spline finite strip method. *Computers and Structures*, 52(2), pp.277-286.

Mohtaram, Y.F., Kahnamouei, J.T., Shariati, M. and Behjat, B., 2011. Experimental and numerical investigation of buckling in rectangular steel plates with groove-shape cut out. *Journal of Zhejiang University*, 13(1), pp.1-14.

Narayanan, R. and Chan, S.L., 1985. Ultimate capacity of plates containing holes under linearly varying edge displacements. *Computers and Structures*, 21(4), pp.841-849.

Paik, J.K., Thayamballi, A.K. and Kim, B.J., 2001. Advanced ultimate strength formulations for ship plating under combined biaxial compression/tension, edge shear, and lateral pressure loads. *Marine Technology*, 38(1), pp.153-164.

Roberts, T.M. and Azizian, Z.G., 1984. Strength of perforated plates subjected to in-plane loading. *Thin-Walled Structures*, 2(2), pp.153-164.

Suneel, K.M., Alagusundaramoorthy, P. and Sundaravadivelu, R., 2007. Ultimate strength of square plate with rectangular opening under axial compression. *Journal of Naval Architecture and Marine Engineering*, 4(7), pp.15-26.

Suneel, K.M., Alagusundaramoorthy, P. and Sundaravadivelu, R., 2009. Interaction curves for stiffened panel with circular opening under axial and lateral loads. *Ships and Offshore Structure*, 4(2), pp.133-143.

Yu, C.L. and Lee J.S., 2012. Ultimate strength of simply supported plate with opening under uniaxial compression. *International Journal of Naval Architecture and Ocean Engineering*, 4(4), pp.423-436.